

Fluctuation and Noise Letters
 © World Scientific Publishing Company

Large Fluctuations in Amplifying Graphs

Stefano Lepri

*Consiglio Nazionale delle Ricerche, Istituto dei Sistemi Complessi,
 Via Madonna del Piano 10 I-50019 Sesto Fiorentino, Italy
 stefano.lepri@isc.cnr.it*

Received (received date)

Revised (revised date)

We consider a model for chaotic diffusion with amplification on graphs associated with piecewise-linear maps of the interval [S. Lepri, *Chaos Sol. Fractals*, **139**,110003 (2020)]. We determine the conditions for having fat-tailed invariant measures by considering approximate solution of the Perron-Frobenius equation for generic graphs. An analogy with the statistical mechanics of a directed polymer is presented that allows for a physically appealing interpretation of the statistical regimes. The connection between non-Gaussian statistics and the generalized Lyapunov exponents $L(q)$ is illustrated. Finally, some results concerning large graphs are reported.

Keywords: Chaotic map, Power-law distributions, Diffusion and amplification on graphs, Generalized Lyapunov exponents

1. Introduction

Large fluctuations are one of the distinctive features of complexity, being associated to lack of a characteristic scale and to extreme events. This work is part of a research program aimed at characterizing large fluctuations caused by the joint effect of energy diffusion and inhomogeneous amplification or growth. Diffusion can originate from underlying disorder and scattering and/or chaotic motion, while growth stems for external energy pumping into the system. This leads to non-Gaussian fluctuations of the relevant physical quantities, whose statistical distributions can have fat-tails, leading to domination of a single event and lack of self-averaging of measurements [1]. This is well-known for multiplicative stochastic processes [2, 3] and chaotic dynamical systems that display intermittency and multifractality [4].

A particularly interesting form of disorder is the one arising in dynamical systems defined on graphs. They have many fascinating and diverse applications to describe complex interacting units with non-uniform connectivity [5]. When heterogeneous reaction is added a non trivial interplay between the connectivity and the local reaction emerges [6].

Among the many possible physical examples, the example we mostly refer to is the one of active, disordered optical media where light amplification and scattering

coexist. [7]. This occurs in random lasers where indeed fat-tailed distributions of emission intensities are observed experimentally [8–13].

This work reviews and extends some of the results of [14] where we introduced a simple dynamical system consisting of a map that couples chaotic diffusion and energy growth and dissipation. Nonlinear maps are time-discrete dynamical models, widely studied to establish the emergence of macroscopic behavior from microscopic chaos [15]. The model is inspired by experiments on *lasing networks* [16,17], consisting of active (lasing) and passive optical fibers supporting many optical modes, excited by external pumping. Optical coupling among the fibers provides a form of topological disorder and the system can be considered, loosely speaking, as a random laser on a graph. Another related experimental setup has been realized with nanophotonic devices by coupling a mesh of subwavelength waveguides [18]. Heuristically, one may think of light as a bunch of rays undergoing chaotic diffusion and (site-dependent) amplification on such graph. As a matter of fact, the classical dynamics of particles on graphs can be described by simple maps. Trajectories of a particle on a graph, undergoing scattering at its vertices, are in one-to-one correspondence with the ones of one-dimensional piecewise chaotic maps [19–21].

The plan of the paper is as follows. In Section 2 we recall and extend the map model introduced [14] along with some examples. In Section 3 we consider an approximate equation for the invariant measure and discuss the conditions for the appearance of the fat-tailed distributions. In Section 4 we examine the symmetries of the problem. Such conditions can be recasted in terms of a statistical mechanics problem: a polymer with a finite number of configurations in a random energy landscape, as described in Section 5. A useful approach is based on generalized Lyapunov exponents as discussed in Section 6. In Section 7 we report explicit analytical results for the simplest case of a two-sites graph. Finally, we extend the analysis to examples of large graphs in Section 8.

2. Graph with diffusion and amplification

We consider the following map [14]

$$\begin{cases} x_{n+1} = f(x_n) \\ E_{n+1} = g(x_n)E_n \end{cases} \quad (1)$$

where $g(x)$ is positive and x_n belongs to the unit interval. The function f is piecewise linear and we assume that the map is chaotic with a Lyapunov exponent $\lambda_1 > 0$. The unit interval is partitioned in N disjoint intervals I_j of equal lengths $1/N$ and we consider a piece-wise constant gain function g ,

$$g(x_n) = g_j \quad \text{for } x_n \in I_j$$

where the constants $g_j \geq 1$ and $0 < g_j < 1$ correspond to local amplification or dissipation respectively. Thus, the "energy" variable E_n is coupled to x_n , leading

to amplification fluctuations. Also, the sequence of multipliers $g(x_n)$ is in one-to-one correspondence with the symbolic dynamics of the map f and has the same time correlation in time. Maps of similar form have been considered in the context of on-off intermittency [22] and synchronization transition of two piecewise-linear chaotic maps [23].

Assuming that the stationary invariant measure $P(x, E)$ of the map is uniform in x , the Lyapunov exponents $\lambda_{1,2}$ are computed straightforwardly

$$\lambda_1 = \int_0^1 \log |f'(x)| dx, \quad (2)$$

$$\lambda_2 = \langle \log(g(x)) \rangle = \frac{1}{N} \sum_j \ln g_j \quad (3)$$

Some specific examples are illustrated in Figure 1 along with their graph representation, constructed by examining the possible transitions in the underlying Markov dynamics. The first two examples f_1, f_2 depend on a parameter p (see Appendix) that controls the transition probabilities and have the same Lyapunov exponent $\lambda_1 = -p \log p - (1-p) \log(1-p)$. Note that $\lambda_1 > 0$ but it is vanishingly small for p approaching 0 and 1 where the maps have weakly-unstable periodic orbits. The third example f_3 , has $\lambda_1 = \log 3$ and corresponds to the case of a complete four-sites graph where transition can occur towards any other site with the same probability. This example can be easily extended to arbitrary N (see Section 8 below).

In the stable case, $\lambda_2 < 0$, the orbits tends to be attracted to the origin while $\lambda_2 > 0$ they are repelled away and tend to grow indefinitely. In order to have a bounded invariant measure one needs to require that the variable E_n neither does drift to infinity nor is stucked at the origin. This can be implemented, for instance, by assuming that there are some "barrier" points located at some prescribed values of E (the scale of E is arbitrary). This can be enforced deterministically: for instance for $\lambda_2 < 0$ setting $E_{n+1} = s$ when $E_n \leq 0$, where s is a small positive number. In this way, E_n is stationary and ranges in $[0, \infty]$. The quantity s is arbitrary, but we anticipate that the main results we are interested in do not depend on its value. ^a In the unstable case, $\lambda_2 > 0$, we may impose the constraint at, say $E = 1$ resetting $E_{n+1} = 1$ whenever $E_n > 1$. Another possibility would be to use stochastic or deterministic resetting, or to allow the trajectories to escape, see [14] for details.

Starting from a "Lagrangian" description in terms of chaotic trajectories we can derive the corresponding "Eulerian" equations for the probabilities. The time-

^aAlso setting the variable to a new randomly chosen variable s_n will do as well, as long as s is very small as it will only affect the shape of the invariant measure close to the boundaries [23]. For a discussion of a similar problem for Langevin dynamics see Ref. [24] and the bibliography therein.

4 Stefano Lepri

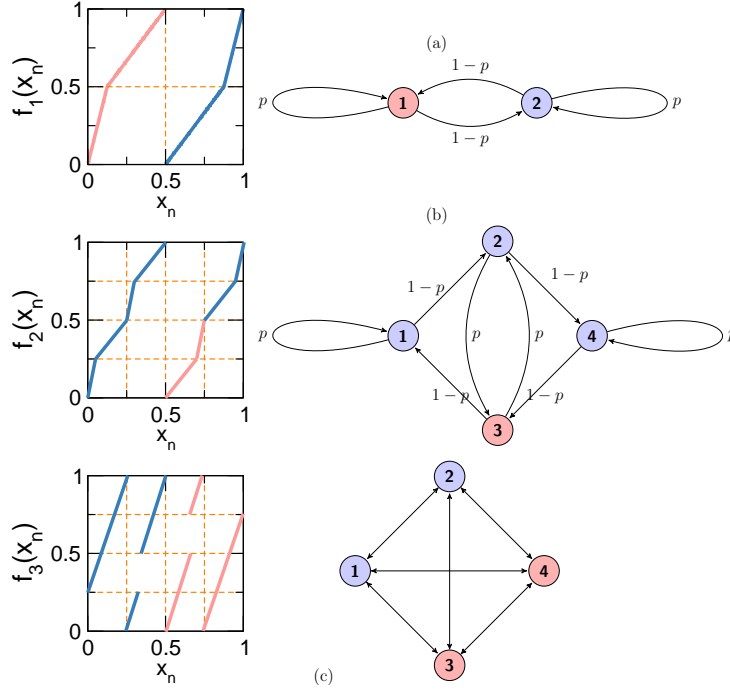


Fig. 1. Left: three examples of the chaotic map and (right) their graph representations. The analytic expressions are given in the Appendix. Red and blue parts represent possible choices of amplifying ($g_j > 1$) and dissipative ($g_j < 1$) regions in phase space.

discrete evolution of the measure $P_n(x, E)$ is solution of Perron-Frobenius operator

$$P_{n+1}(x, E) = \sum_j \frac{1}{g_j |f'(y_j)|} P_n \left(y_j, \frac{E}{g_j} \right) \quad (4)$$

where $y_j(x) = f^{-1}(x)$ are the N pre-images of x . Boundary conditions are required to specify $P_n(x, E)$ to take properly into account the barrier points.

To give an idea of the dynamics, we report in Figure 2 some representative trajectories for the map f_2 along with the attractors in phase space and histograms of the variable $z = \log E$. Note that an exponential decay at large z is a signature of a power-law tail in the variable E , that occurs when large fluctuations arise.

3. Fast chaotic diffusion

Since we are interested in the statistical properties of E , it is natural to consider, in view of definition of $g(x)$, the probabilities $P_{j,n}(E)$ to have a particle with energy E in each interval I_j . In general, it is not possible to write a closed equation for the $P_{j,n}$ from (4). A simplified case is when the Lyapunov exponent λ_1 is much larger than the typical rate of change of the energy variable. If so, we may assume that

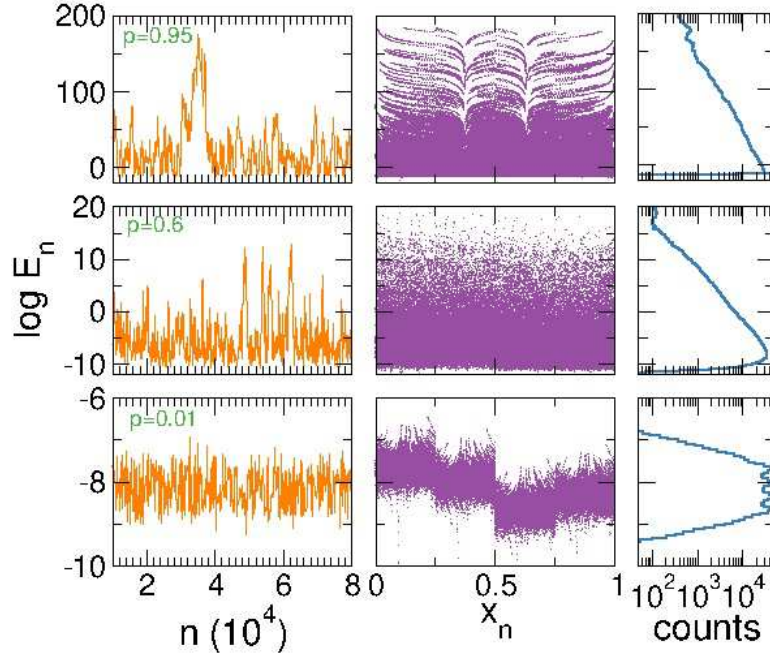


Fig. 2. Time evolution and statistics of iterates of the map f_2 given in Fig.1 for $p = 0.95, 0.6, 0.01$ (bottom to top). The gain factors are $g_{1,2,4} = 0.7$, $g_3 = 2.7$, corresponding to the Lyapunov exponent $\lambda_2 \approx -0.0192$. Left panels: trajectory snapshots, middle column: distribution of the iterates in phase space $(x_n, \log E_n)$, histograms of the variable $\log E_n$ in semi-logarithmic scale.

the measure becomes rapidly uniform in x within each interval I_j . We can thus look for solutions of (4) independent of x ,

$$P_{i,n+1}(E) = \sum_j \frac{W_{ij}}{g_j} P_{j,n} \left(\frac{E}{g_j} \right) \quad (5)$$

Then W is the $N \times N$ stochastic matrix for a random walk on a N -sites, directed graph. In our case the transition probabilities are given by the inverses of the map slopes (see the leftmost part of Figure 1 and the Appendix); W is symmetric and doubly stochastic, $\sum_j W_{j,i} = \sum_j W_{i,j} = 1$. This defines a Markov process in discrete time, as better seen by recasting (5) in the mathematically equivalent form

$$P_{i,n+1}(E) = \sum_j \int K_{i,j}(E, E') P_{j,n}(E') dE'$$

$$K_{i,j}(E, E') = W_{ij} \delta(E - g_j E'),$$

that defines the transition rates $K_{ij}(E, E')$ (this last equation reduces to (5) by integrating the δ s). We also mention in passing that a Kramers-Moyal expansion, suitable when all the g_j are close to unity, allows to derive a set of coupled Langevin

6 *Stefano Lepri*

equations for the energies at each graph site. The details of the derivation will be reported elsewhere. Such equation contain *stochastic advection* terms, akin to the one found in the lattice case [25].

4. Fat-tailed distributions

Let us now examine the possibility of having sower-law solutions in the steady state $P_{i,n}(E) = P_i(E)$ of the form $P_i = Q_i E^{-\beta-1}$; with $\beta > 0$ for normalizability. The Q_i are the marginal probabilities to be on site i with whatever energy. Substituting this Ansatz in the stationarity condition we obtain a consistency condition for β

$$Q_i = \sum_j W_{ij} g_j^\beta Q_j \quad (6)$$

i.e. Q must be an eigenvector of eigenvalue one of the matrix $W_{ij} g_j^\beta$, i.e.

$$\det(WG^\beta - 1) = 0, \quad (7)$$

where G is a diagonal matrix having elements g_j . Note that $\beta = 0$ is always a solution. Moreover, the condition is invariant under the transformations

$$g_j \longrightarrow \frac{1}{g_j}, \quad \beta \longrightarrow -\beta. \quad (8)$$

This should be interpreted as follows. If there exist a distribution decaying for large E as $E^{-\beta-1}$ in the stable case $\lambda_2 < 0$, then the distribution in the unstable case with Lyapunov exponent $-\lambda_2$ is $E^{\beta-1}$ for small E (up to a cutoff set by the upper barrier).

The more interesting regime occurs for $|\beta| < 2$ where the measures have diverging variance (up to the barrier cutoff). Here, we expect a strongly intermittent dynamics, with dominance of single large fluctuations on the average, as in the well-know case of Lévy-stable distributions [26]. For a fixed W , the region in the N -dimensional parameter space (g_1, \dots, g_N) where this occurs, is thus bounded between the hyper-surfaces defined by the condition (7) with $\beta = \pm 2$ (see Section 7 for an example).

5. Statistical mechanics analogy

Let us now show that finding a power-law decay of the measure can be interpreted as dual statistical mechanics problem. First, Equation (7) can be rewritten in an equivalent manner by imposing that the symmetrized matrix $g_i^{\beta/2} W_{ij} g_j^{\beta/2}$ has an eigenvalue equal to one. Let us define the quantities h_j and E_{ij}

$$\ln g_j = \lambda_2 + h_j; \quad E_{ij}(\beta) = -\frac{1}{\beta} \ln W_{ij} - \frac{h_i + h_j}{2}$$

with $\sum_j h_j = 0$ and λ_2 is defined by (3). We can thus rephrase the problem in terms of the statistical mechanics of a directed polymer of length ℓ whose microscopic

configurations are labeled by sequences of $\sigma_1, \sigma_2 \dots \sigma_\ell$, with σ_i being an integer assuming values $\sigma_i = 1, 2 \dots, N$. The polymer energy is

$$H = \sum_i E_{\sigma_i, \sigma_{i+1}}. \quad (9)$$

The quantity E_{ij} thus represents the energy cost between two consecutive beads of the polymer. It consist of two terms: the one dependent on W is a kind of elastic energy, while the h_j represent some local energies, akin to the case of the polymer on a disordered substrate [27]. Larger positive values of h_j correspond to stronger interaction with the substrate itself. ^b To obtain a thermodynamic state one has to impose some upper and lower bounds to the polymer energy in the same way done in the map model.

The standard approach to compute the partition function associated with H , is to introduce the $N \times N$ transfer matrix

$$T(\sigma_1, \sigma_2) = \exp[-\beta E_{\sigma_1, \sigma_2}];$$

and β is interpreted as the inverse temperature. As it is well known, the partition function of the polymer of length ℓ is the trace of T^ℓ or, equivalently, the sum of the eigenvalues τ_i of T , $\sum_i \tau_i^\ell$. For large ℓ , we thus have to impose that its free energy, namely its the maximal eigenvalue is equal to $\exp(-\beta\lambda_2)$,

$$\beta\lambda_2 = -\log \tau_1. \quad (10)$$

This condition is indeed equivalent to (6) or (7). Notice that, considering the model parameters as fixed, this it is a kind of inverse procedure with respect to the standard case: one fixes the free energy and wants to determine the corresponding temperature. By virtue of the Perron-Frobenius theorem since the matrix T is strictly positive then the leading eigenvalue τ_1 is strictly positive and non degenerate. Also for a finite N it an analytic function of the element so there are no phase transitions.

The analogy is also suggestive to understand the difference between the fat-tailed and Gaussian regimes. As said, the first case corresponds to $0 < \beta < 2$. In the polymer language, this would correspond to the high-temperature regime where the elastic energy terms dominate on the pinning terms. In other words, the polymer is very stiff and the typical lowest-energy configurations will be trapped close to the largest h_j . These configurations give large fluctuations above the average in agreement with the above point of view. On the contrary, for low temperatures the polymer is very loose, and explores the whole configuration space at low cost, making deviations from the average behavior very unlikely. In this respect the value $\beta = 2$ can be consider to define the characteristic temperature where the two energy terms balance.

^bOtherwise it could be represented as a chain of N -components spins. Here, the spin variables σ_i take values in the set $1, 2, \dots, N$ on each site and h_i is a spin-dependent constant magnetic field. In this interpretation it is reminiscent of the Potts model with nearest-neighbor interactions in 1d. It is different from the simple standard case where the interaction is of the form $\delta_{\sigma_i, \sigma_{i+1}}$.

Since $\tau_1 > 0$, equation (10) has no solution for $\lambda_2 > 0$, and hence to thermodynamically stable states for the polymer problem in the canonical ensemble, as formulated so far. This correspond to the fact that for the dynamical system the origin is unstable. To account for this case, one can reason in two ways. One is to consider positive temperature states of a modified Hamiltonian $-H$, exploiting the symmetry (8). Alternatively, a more suggestive thermodynamic interpretation is in terms of *negative absolute temperature*. Let us consider the microcanonical states of the polymer with Hamiltonian H at total energy E . Then all the microscopic configurations are precisely those that reach such such energy. Upon increasing λ_2 the number of such configurations, and thus the polymer entropy $S(E)$, should decrease leading to negative temperature from the usual relation $\beta = \partial S / \partial E$. Following the standard reasoning, we can thus regard the unstable regime as microcanonical state with negative absolute temperature where ensemble equivalence does not hold. [28].

6. Generalized Lyapunov exponents

A general and elegant approach to look at the problem of fat-tails is from the point of view of large deviation of Lyapunov exponents [31]. For the dynamical system like (1) one can consider the generalized Lyapunov exponents $L(q)$, that are the growth rates of the q th moment of the perturbation as $\exp(L(q)\tau)$ at large times τ [4, 30, 31]. The $L(q)$ is the cumulant generating function of the associated variable and contains all the information on the fluctuations beyond the Gaussian regimes [32, 33]. The standard Lyapunov exponent is given by $\lambda_2 = L'(q = 0)$, and corresponds to the typical average growth of a fluctuation. Thus, deviations of $L(q)$ from a linear behavior, $\lambda_2 q$, are a signature of intermittent dynamics [34]. The existence of power-law stationary tails can be inferred from inspection of the behavior of the $L(q)$ [23, 35, 36]. Indeed, if $L(q) > 0$ for large enough q then there is a finite probability for a small perturbation to grow very large with respect to the average. More precisely, the condition for power-law distributions with a diverging moments for $q > q_*$ is that $L(q_*) = 0$ [23, 35]. Such condition must be equivalent to (7), namely a distribution decaying as E^{-1-q_*} , i.e. $q_* = \beta$. Also, the boundaries of the region with fat-tailed distribution are defined by $L(\pm 2) = 0$.

For the master equation (5), the generalized exponents can be computed exactly from equations (11). To this aim, we consider the equation *without barrier boundary conditions* and consider the moments of E in each portion I_i of the unit interval,

$$\epsilon_{i,n}^{(q)} \equiv \int E^q P_{i,n}(E) dE.$$

By multiplying equation (5) by E^q and integrating in dE , we straightforwardly obtain a set of N difference equations

$$\epsilon_{i,n+1}^{(q)} = \sum_j W_{ij} g_j^q \epsilon_{j,n}^{(q)} \quad (11)$$

that are linear and closed at each order (moments of different order q are decoupled). Using the same notation as above, this amounts simply to compute the largest

eigenvalue of the matrix WG^q and evaluate $L(q)$ as the logarithm of it, a procedure that is basically the same followed to compute the cumulant generating function of Markovian dynamics [37]. Note that the matrix can be made symmetric by the same transformation as given at the beginning of Section 5, so the eigenvalues are real. Also, comparing with (8), we see that the spectrum of generalized exponents is also invariant under the transformation $g_j \rightarrow 1/g_j$ and $q \rightarrow -q$, which is related to the time-reversal invariance of the trajectories of the map.

For general graphs the eigenvalues can be easily computed numerically. In Figure 3 we report the exponents for the case of the map f_2 . It is known that the exponents are notoriously hard to compute especially for large q values that requires sampling very unlikely trajectories [38, 39]. We thus profit to test the accuracy of the direct method, with respect to the one based on computation of the eigenvalues. As seen from the data, for this simple example the direct method is in reasonable agreement, meaning that sampling accuracy is not a big issue in those examples.

This approach is also accurate in reproducing the measured exponents $\pm\lambda_2$. For instance, as a numerical test for the case $p = 0.6$ of Figure 4, the condition $L(q_*) = 0$ yields $q_* \approx 0.225$. to be compared from the fit of the distribution of $z = \log E$ yielding $\exp(-0.223z)$ for large z (see [14] for further numerical checks).

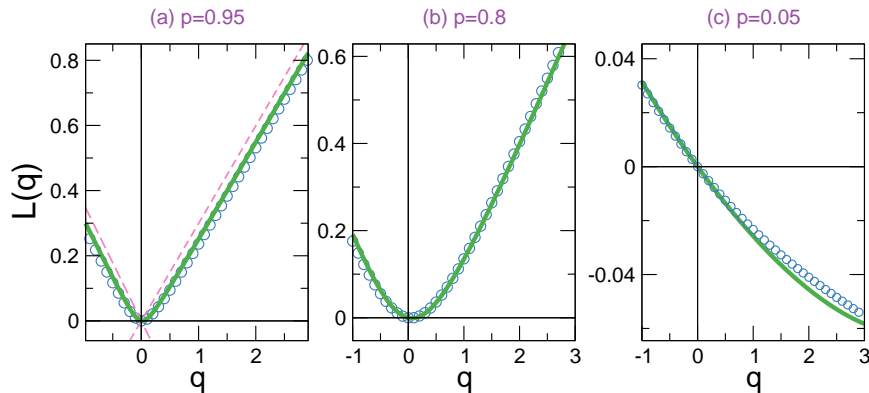


Fig. 3. The generalized Lyapunov exponents $L(q)$ for the map f_2 and for different values of parameter p and $g = 1.2$ $l = 0.8$. Symbols are the numerical values computed via the definition, for an ensemble of trajectories of finite duration $t = 20$ (a,b) and $t = 160$ (c); solid lines are the $L(q)$ computed as the logarithm of the largest eigenvalue of the matrix WG^q (see text). In the case $p = 0.95$, we also draw the lines corresponding to the maximal and average growth rates, $q \log l$ and $\lambda_2 q$.

In Figure 4a we compare two cases having parameters g_j and $1/g_j$ and thus opposite Lyapunov exponents. According to (8) the statistics of should have opposite rates $\exp(\pm q_* z)$, as well verified by the data. It is also seen that the large fluctuation has a form of statistical symmetry, in the sense that their shape E_n for

10 *Stefano Lepri*

$\lambda_2 < 0$ would be similar to $1 - E_n$ for $\lambda_2 < 0$. (see Figure 4b) Moreover, rise and fall rates are accurately predicted by $L'(q_*)$ and λ_2 , respectively, as read from Figure 4c.

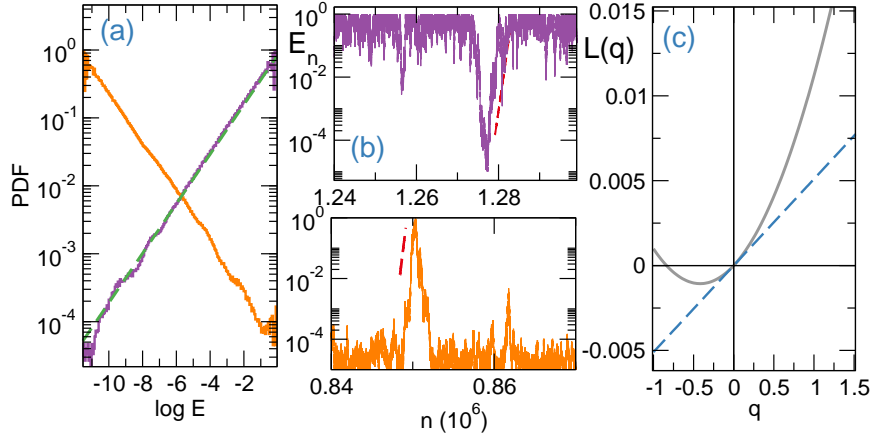


Fig. 4. Comparison between the cases with opposite Lyapunov exponents $\pm\lambda_2$ for the map f_2 with $p = 0.5$, $g_1 = g_3 = g_4 = 0.9$, $g_1 = 1.4$ (orange curves) and $g_1 = g_3 = g_4 = 1/0.9$, $g_1 = 1/1.4$ and (purple). Panel (a): distributions of $z_n = \log E_n$, the dashed line is the expected exponential behavior $\exp(-q_* z)$ where $q_* = -0.84$ is the given by $L(q_*) = 0$. Panels (b): time series of E_n showing the build and decay of a large fluctuation: the dashed lines correspond to exponential growth/decay according to $\exp(\lambda_2 t)$ with $\lambda_2 = 5.09 \cdot 10^{-3}$. Panel (c): the generalized Lyapunov exponents $L(q)$ (solid line) for the case $\lambda_2 > 0$, the dashed line is $\lambda_2 q$.

7. Two-sites graph: analytical solutions

For the simplest case of the two-sites graph, corresponding to the map f_1 in Figure 1 some explicit analytical results can be worked out. The stationary measure is solution of (letting $g_1 = g$, $g_2 = l$).

$$\begin{aligned} P_1(E) &= \frac{p}{g} P_1\left(\frac{E}{g}\right) + \frac{1-p}{l} P_2\left(\frac{E}{l}\right) \\ P_2(E) &= \frac{(1-p)}{g} P_1\left(\frac{E}{g}\right) + \frac{p}{l} P_2\left(\frac{E}{l}\right). \end{aligned} \quad (12)$$

- The consistency conditions, Eq. (7) yields

$$\det(WG^\beta - 1) = -p(g^\beta + l^\beta) + (2p - 1)g^\beta l^\beta + 1 = 0 \quad (13)$$

where the transition matrix is given by W_1 in (19) and $G^\beta \equiv \begin{pmatrix} g^\beta & 0 \\ 0 & l^\beta \end{pmatrix}$.

The region in the (g, l) with large fluctuations $|\beta| < 2$ is bounded between the curves defined by (13) with $\beta = \pm 2$.

- The statistical mechanics analogy can be worked out explicitly in the "spin" interpretation as an Ising chain. Let $g = \exp(\lambda_2 + h)$, $l = \exp(\lambda_2 - h)$ in (13), the transfer matrix coincides with the well-known textbook expression of the one-dimensional Ising model with β dependent parameters

$$H = \sum_i [-J\sigma_i\sigma_{i+1} + h\sigma_i]$$

($\lambda_2 \equiv \lambda$). Upon letting

$$p = \frac{e^{\beta J}}{e^{\beta J} + e^{-\beta J}}; \quad 1 - p = \frac{e^{-\beta J}}{e^{\beta J} + e^{-\beta J}}; \quad J(\beta) = \frac{1}{2\beta} \ln\left(\frac{p}{1-p}\right)$$

condition (10) is rewritten in the familiar form

$$\exp(-\beta\lambda) = e^{\beta J} \cosh \beta h + \sqrt{e^{2\beta J} \sinh^2 \beta h + e^{-2\beta J}}$$

Also, it gives a nice interpretation of the parameter p . The very definition of J makes transparent that p is interpreted as a probability of a spin-flip and controls the type of interaction. In particular:

- for $p = 1/2$: $J = 0$ and

$$\beta\lambda = -\ln \cosh \beta h$$

that correspond to 1d Ising paramagnet in external field h

- For $1/2 < p < 1$: $J > 0$ ferromagnetic interaction;
- For $0 < p < 1/2$: $J < 0$ antiferromagnetic interaction.

In this language, the variable of interest is the magnetic energy of the spin chain.

- Generalized Lyapunov exponents can be computed analytically as described above yielding [14]

$$L(q) = \log \left| \frac{p(g^q + l^q) + \sqrt{p^2(g^q + l^q)^2 - 4(2p-1)g^q l^q}}{2} \right|. \quad (14)$$

and it can be checked that the condition $L(q_*) = 0$ yields the same as (13).

In Fig. 5 we summarize the various statistical regimes of the model, distinguishing the parameters values where fluctuations have diverging variance.

8. Large graphs

So far we have considered graphs with a small number of sites. A natural question would be how the result change upon increasing N , in particular whether the fat-tailed regimes persist. This is not an obvious question. For instance in large chaotic systems, the generalized Lyapunov exponents may become proportional to q . The heuristic explanation is that, due to fast correlation decay in spatio-temporal chaos, the norm vector is the sum of entries that grow almost independently [30]. In the

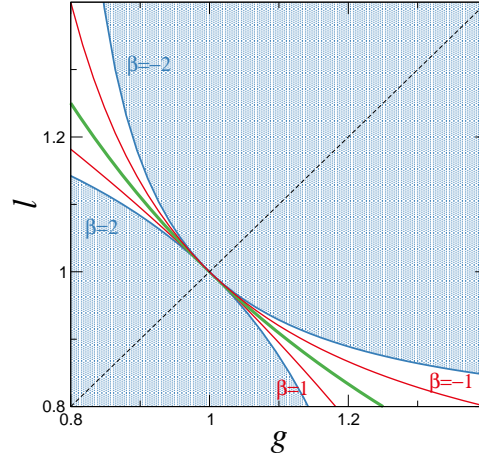


Fig. 5. Phase diagram in the parameter plane (g, l) for two-sites graph, corresponding to the map f_1 in Figure 1 with $p = 0.6$. The green line is the bifurcation line where $\lambda_2 = 0$. There is an obvious reflection symmetry around the line $g = l$ (black dashed). Shaded blue regions correspond to finite variance of the variable E_n yielding Gaussian fluctuations. The region bounded between the curves with $\beta = \pm 2$ is where Lévy-like fluctuations are expected.

present example however the multipliers g_j are quenched and the situation may be different.

For simplicity, let us discuss directly the Markovian dynamics, Eq. (5). As a first instance, let us consider the ladder graph composed of $N = 2M$ sites depicted in Fig. 6. For convention, we label the upper sites with even integers and the lower by odd ones. The transition matrix has non-zero elements given by

$$W_{2i,2(i+1)} = W_{2i+1,2i-1} = p; \quad W_{2i,2i+1} = W_{2i+1,2i} = 1 - p \quad (15)$$

for $i = 1 \dots M$, and $W_{ij} = 0$ otherwise. Periodic boundaries have been assumed. This is a geometry which can be seen as an extension of the map f_2 discussed above.

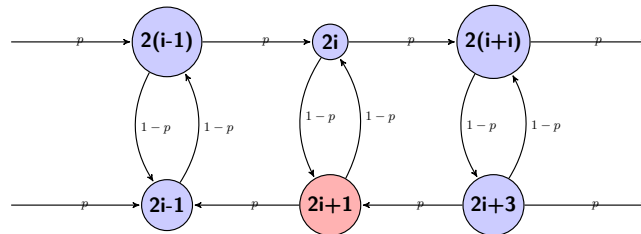


Fig. 6. The ladder graph described by the transition matrix (15). Configuration with only one active site, labeled by red color.

Another example is the complete graph

$$W_{i,i} = 0; \quad W_{i,j} = \frac{1}{N-1} \quad i \neq j \quad (16)$$

which is depicted in the lowest panel of Fig. 1 for $N = 4$. For simplicity, let us consider also the case of a single active site with all the other having equal dissipation, namely $g_j = g > 1$ for a certain $j = j_0$ and $g_j = l < 1$ otherwise. With such choice, the Lyapunov exponent is $\lambda_2 = (1 - 1/N) \log l + (\log g)/N$ in both examples, and approaches the constant value $\lambda_2 \approx \log l < 0$ for N large.

In Fig. 7 we compare the generalized Lyapunov exponents (computed as above) for the two graphs for increasing size N . In the case of the ladder, the $L(q)$ are N -independent and the example shown predicts that a fat-tail with $q_* \approx 1$ should persist upon increasing the size. On the contrary for the complete graph q_* grows with N suggesting that the statistics should turn Gaussian for large enough N .

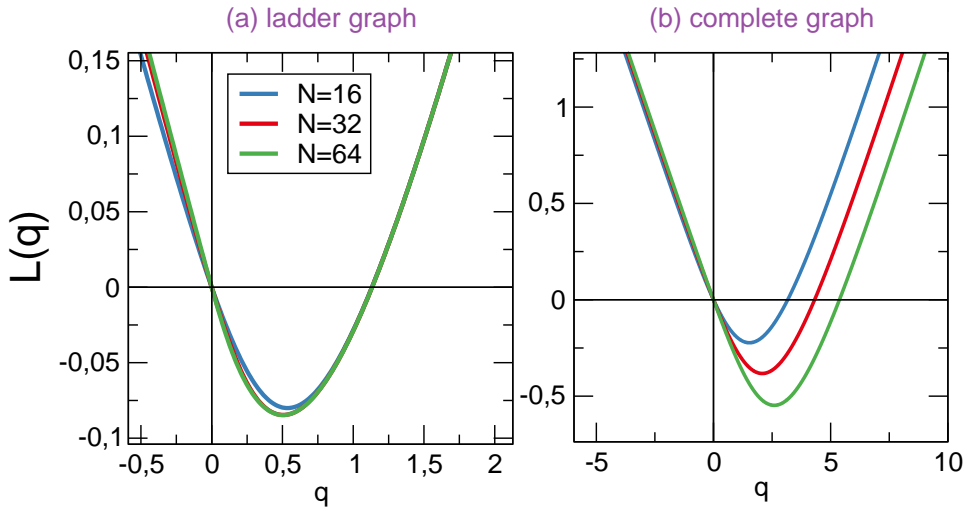


Fig. 7. The generalized Lyapunov exponents $L(q)$ for (a) the ladder graphs and (b) the complete graph and different number of sites N ; $p = 0.4$ $g_3 = 3.0$ and $g_j = 0.7$ for $j \neq 3$.

This is qualitatively consistent with the polymer interpretation, Equation (9). In the ladder case the elastic energy of the polymer is independent of the size. On the contrary for the complete graph the elastic energy decreases with N making the polymer more and more loose and hindering the observation of configurations associated with large energy fluctuations.

9. Conclusion

Motivated by experiments on active, disordered optical systems, we have studied a map model that combines chaotic diffusion and amplification on a graph [14].

Within a stochastic approximation of the dynamics, given by the Markov process described by (5), we established the conditions for its invariant measure to display fat-tailed distributions in some regime of parameters. We mostly discussed some specific small graphs ($N = 2, 4$) examples and extended the results to large graphs (ladder and complete). The model has symmetries that allows to consider the stable and unstable cases in a simple way. Also, the problem can be interpreted in statistical mechanics language, an analogy that can be fruitful to interpret the dynamical regimes. We have confirmed that the Generalized Lyapunov exponents provide a useful and simple tool to predict the fluctuation statistics and the anatomy of a large fluctuation, both in the stable and unstable cases. The model has its own interest but is also a guidance for interpretation of experiments in the optical disordered media as for instance the lasing networks [17].

Acknowledgements

The Author acknowledges S. Iubini, A. Politi and P. Politi for useful discussions and A. Di Garbo and R. Mannella for the invitation to the workshop DCP22 in Pisa.

Appendix

For reference we give here the functional forms of the examples considered in Fig. 1:

$$f_1(x) = \begin{cases} \frac{1}{p}x & 0 \leq x \leq p/2 \\ \frac{1}{1-p}x + \frac{1-2p}{2(1-p)} & p/2 < x \leq 1/2 \\ \frac{1}{1-p}x - \frac{1}{2(1-p)} & 1/2 < x \leq 1 - p/2 \\ \frac{1}{p}x + 1 - \frac{1}{p} & 1 - p/2 < x \leq 1 \end{cases} \quad (17)$$

$$f_2(x) = \begin{cases} x/p & x < p/4 \\ (x - p/4)/(1 - p) + 1/4 & p/4 \leq x < 1/4 \\ (x - 1/4)/p + 1/2 & 1/4 < x < 1/4 + p/4 \\ (x - 1/4 - p/4)/(1 - p) + 3/4 & 1/4 + p/4 < x < 1/2 \\ (x - 1/2)/(1 - p) & 1/2 < x < 3/4 - p/4 \\ (x - 3/4 + p/4)/p + 1/4 & 3/4 - p/4 < x < 3/4 \\ (x - 3/4)/(1 - p) + 1/2 & 3/4 < x < 1 - p/4 \\ (x - 1 + p/4)/p + 3/4 & 1 > x > 1 - p/4 \end{cases} \quad (18)$$

where $0 \leq p \leq 1$. The stochastic matrices used in the text are

$$W_1 \equiv \begin{pmatrix} p & 1-p \\ 1-p & p \end{pmatrix}, \quad W_2 \equiv \begin{pmatrix} p & 1-p & 0 & 0 \\ 0 & 0 & p & 1-p \\ 1-p & p & 0 & 0 \\ 0 & 0 & 1-p & p \end{pmatrix} \quad (19)$$

while for f_3 is given by (16) for $N = 4$.

References

- [1] J.-P. Bouchaud and A. Georges, “Anomalous diffusion in disordered media: statistical mechanisms, models and physical applications”, *Physics reports* **195** (1990) 127–293.
- [2] D. Sornette, “Multiplicative processes and power laws”, *Physical Review E* **57** (1998) 4811.
- [3] J. García-Ojalvo and J. Sancho, *Noise in spatially extended systems* (Springer Verlag, 1999).
- [4] A. Crisanti, G. Paladin and A. Vulpiani, *Products of random matrices in statistical physics*, volume 104 (Springer Science & Business Media, 2012).
- [5] M. A. Porter and J. P. Gleeson, *Dynamical Systems on Networks: A Tutorial* (Springer series Frontiers in Applied Dynamical Systems: Reviews and Tutorials, Switzerland, 2016).
- [6] G. Cencetti, F. Battiston, D. Fanelli and V. Latora, “Reactive random walkers on complex networks”, *Physical Review E* **98** (2018) 052302.
- [7] D. S. Wiersma, “The physics and applications of random lasers”, *Nat. Phys.* **4** (2008) 359–367.
- [8] S. Lepri, S. Cavalieri, G. Oppo and D. S. Wiersma, “Statistical regimes of random laser fluctuations”, *Phys. Rev. A* **75** (2007) 063820.
- [9] S. Lepri, “Fluctuations in a diffusive medium with gain”, *Phys. Rev. Lett.* **110** (2013) 230603.
- [10] E. Raposo and A. Gomes, “Analytical solution for the Lévy-like steady-state distribution of intensities in random lasers”, *Phys. Rev. A* **91** (2015) 043827.
- [11] E. Ignesti, F. Tommasi, L. Fini, S. Lepri, V. Radhakshmi, D. Wiersma and S. Cavalieri, “Experimental and theoretical investigation of statistical regimes in random laser emission”, *Phys. Rev. A* **88** (2013) 033820.
- [12] R. Uppu and S. Mujumdar, “Lévy exponents as universal identifiers of threshold and criticality in random lasers”, *Phys. Rev. A* **90** (2014) 025801.
- [13] A. S. Gomes, E. P. Raposo, A. L. Moura, S. I. Fewo, P. I. Pincheira, V. Jerez, L. J. Maia and C. B. De Araújo, “Observation of Lévy distribution and replica symmetry breaking in random lasers from a single set of measurements”, *Scientific reports* **6** (2016) 27987.
- [14] S. Lepri, “Chaotic fluctuations in graphs with amplification”, *Chaos, Solitons & Fractals* **139** (2020) 110003.
- [15] R. Klages, *Microscopic chaos, fractals and transport in nonequilibrium statistical mechanics*, volume 24 (World Scientific, 2007).
- [16] S. Lepri, C. Trono and G. Giacomelli, “Complex active optical networks as a new laser concept”, *Physical review letters* **118** (2017) 123901.
- [17] G. Giacomelli, S. Lepri and C. Trono, “Optical networks as complex lasers”, *Physical Review A* **99** (2019) 023841.
- [18] M. Gaio, D. Saxena, J. Bertolotti, D. Pisignano, A. Camposeo and R. Sapienza, “A nanophotonic laser on a graph”, *Nature communications* **10** (2019) 1–7.
- [19] F. Barra and P. Gaspard, “Classical dynamics on graphs”, *Phys. Rev. E* **63** (2001) 066215.
- [20] G. Tanner, “Spectral statistics for unitary transfer matrices of binary graphs”, *Journal of Physics A: Mathematical and General* **33** (2000) 3567.
- [21] P. Pankowski, K. Zyczkowski and M. Kus, “Classical 1d maps, quantum graphs and ensembles of unitary matrices”, *J. Phys. A* **34** (2001) 9303.

- [22] H. Fujisaka, H. Ishii, M. Inoue and T. Yamada, “Intermittency caused by chaotic modulation. ii: Lyapunov exponent, fractal structure and power spectrum”, *Progress of theoretical physics* **76** (1986) 1198–1209.
- [23] A. S. Pikovsky and P. Grassberger, “Symmetry breaking bifurcation for coupled chaotic attractors”, *Journal of Physics A: Mathematical and General* **24** (1991) 4587.
- [24] H. Nakao, “Asymptotic power law of moments in a random multiplicative process with weak additive noise”, *Physical Review E* **58** (1998) 1591.
- [25] S. Lepri, “Fluctuations in a diffusive medium with gain”, *Physical review letters* **110** (2013) 230603.
- [26] V. V. Uchaikin and V. M. Zolotarev, *Chance and stability: stable distributions and their applications* (Walter de Gruyter, 1999).
- [27] J. Krug, “Origins of scale invariance in growth processes”, *Advances in Physics* **46** (1997) 139–282.
- [28] M. Baldovin, S. Iubini, R. Livi and A. Vulpiani, “Statistical mechanics of systems with negative temperature”, *Physics Reports* **923** (2021) 1–50.
- [29] H. Touchette, “Introduction to dynamical large deviations of Markov processes”, *Physica A: Statistical Mechanics and its Applications* **504** (2018) 5–19.
- [30] A. Crisanti, G. Paladin and A. Vulpiani, “Generalized Lyapunov exponents in high-dimensional chaotic dynamics and products of large random matrices”, *Journal of statistical physics* **53** (1988) 583–601.
- [31] A. Pikovsky and A. Politi, *Lyapunov exponents: a tool to explore complex dynamics* (Cambridge University Press, 2016).
- [32] H. Schomerus and M. Titov, “Statistics of finite-time Lyapunov exponents in a random time-dependent potential”, *Physical Review E* **66** (2002) 066207.
- [33] R. Zillmer and A. Pikovsky, “Multiscaling of noise-induced parametric instability”, *Physical Review E* **67** (2003) 061117.
- [34] R. Benzi, G. Paladin, G. Parisi and A. Vulpiani, “Characterisation of intermittency in chaotic systems”, *Journal of Physics A: Mathematical and General* **18** (1985) 2157.
- [35] J. M. Deutsch, “Generic behavior in linear systems with multiplicative noise”, *Phys. Rev. E* **48** (1993) 4179–4182.
- [36] J. M. Deutsch, “Probability distributions for multicomponent systems with multiplicative noise”, *Physica A* **208** (1994) 445–461.
- [37] H. Touchette, “The large deviation approach to statistical mechanics”, *Physics Reports* **478** (2009) 1–69.
- [38] J. Vanneste, “Estimating generalized Lyapunov exponents for products of random matrices”, *Physical Review E* **81** (2010) 036701.
- [39] C. Anteneodo, S. Camargo and R. O. Vallejos, “Importance sampling with imperfect cloning for the computation of generalized Lyapunov exponents”, *Physical Review E* **96** (2017) 062209.